Polímeros
ISSN 1678-5169 (Online)

https://doi.org/10.1590/0104-1428.20240089

ORIGINAL ARTICLES

Contemporary methods of industrial composite material production technology

Andrii Bieliatynskyi[1], Olena Bakulich[2], Viacheslav Trachevskyi[3]* and Mingyang Ta[1]

[1]School of Civil Engineering, North Minzu University, Yinchuan, NingXia, P.R. China
[2]Faculty of Management, Logistic and Tourism, National Transport University, Kyiv, Ukraine
[3]Institute of Chemistry of High-Molecular Compounds, National Academy of Sciences of Ukraine, Kyiv, Ukraine
**viacheslav.trachevskyi@edu-knu.com; meches49@ukr.net*

Abstract

Composite materials have emerged as a viable alternative to metals due to their lighter weight and superior mechanical properties; however, due to the trade-off between performance and cost, they have yet to gain widespread adoption. Despite environmental legislation constantly being updated, producers of various equipment and structures are hesitant to incorporate composite technologies into standard constructions and products, primarily for economic reasons. As a consequence, recent advancements in composite-producing processes have focused on the usage of carbon composites and automated robotics incorporation for ecologically conscious, stable, and affordable production. Therefore, it is essential to investigate current methodologies for industrial carbon composite material production and manufacturing processes to determine the most optimal composite production and implementation criteria.

Keywords: *binders, composite materials, fibrous filler, carbon nanotubes.*

How to cite: Bieliatynskyi, A., Bakulich, O., Trachevskyi, V., & Ta, M. (2025). Contemporary methods of industrial composite material production technology. *Polímeros: Ciência e Tecnologia*, *35*(2), e20250022. https://doi.org/10.1590/0104-1428.20240089

1. Introduction

Matrix and filler materials can be of the most diverse nature and origin. The filler serves as a reinforcing element in composite materials and has significantly higher physical and mechanical properties than the matrix. The composites' specific mechanical properties are noticeably higher than the initial components. Composites differ from filled polymer systems in that the role of the filler is reduced to lowering the price of the final product while the mechanical properties of the material are noticeably increased[1,2]. Despite public distrust of ultra-light modern composites, carbon and other fibrous composites are becoming commonplace when structural materials require high stiffness and low weight, along with corrosion resistance and impact and fatigue resistance[3].

Fiber composites are the most famous examples of modern composites, characterized by high strength, high stiffness, and low weight. A high melting point, coefficient of thermal expansion, and low density also characterize these materials, which are desirable technical properties. In construction, structure weight is crucial since it should support a given load and do so with a minimum of elastic deflection. Thus, strength fibers are compared based on specific modulus and specific strength, i.e., modulus or strength divided by density, respectively. In this case, plastics (polyethylene, aramid fiber) and glass are the stiffest materials, while metals show low indicators of specific stiffness and specific strength. However, using fibers directly is impossible; they should be bonded with a matrix[4,5]. Fibers can be randomly arranged in a plane or in three dimensions, but such an arrangement reduces the possible density of the fiber structure. Fibers are also woven into mats before being incorporated into the composite because this makes it easier to work with fiber arrays[6].

The anisotropy of properties of fiber composites is design engineering using advanced composites. Anisotropy can vary; fibers can be placed exactly where they are needed in a structure to support loads. It is also possible, for example, to vary the amount and orientation of fibers along the length of the beam to vary the stiffness and torsional stiffness of the material[7]. If computer techniques had not been invented, it would be impossible to exploit the advantages of anisotropic materials, such as carbon fiber-reinforced plastics. Due to the complexities and large number of variables involved, computer programs are required to relate the characteristics of individual lamellae to the properties of the fibers and to account for interactions in terms of bending-torsion coupling between different lamellae. Originally, engineers were dissatisfied with the anisotropy of the material, so these complexities were viewed as a significant disadvantage, but this issue found its solution[8].

The unique properties of carbon structural modifications discovered in the second half of the 20th century have captivated researchers. The unique structure and quantum size

effects of nanoscale carbon materials (graphene, fullerenes, single-walled carbon nanotubes, nanoscale diamond, etc.) define their exceptional properties, including a large specific surface area, high strength, electrical conductivity, and the ability to incorporate diverse functional groups[9]. The listed factors open up possibilities for using carbon nanomaterials to modify and create new composites with reinforced properties.

Currently, one of the primary applications of carbon nanoscale fillers is the development of composite materials, including next-generation polymer composite materials (hereafter – PCM) with enhanced physical, mechanical, operational, and functional properties[10-18]. The ability to reduce weight while maintaining high operational characteristics is a critical factor influencing technology's competitiveness. In this regard, there are many opportunities for using PCMs made primarily of carbon fibers. As a result, the challenge of imbuing PCMs with the functional physical and mechanical properties of nanoscale fillers while retaining the matrix's operational characteristics is highly relevant.

Based on a brief examination of the problems associated with the production of modern composite materials, the aim of this research is to develop a modern method of producing industrial composite materials.

2. Materials and Methods

The development and study of composites, which are polymers filled with nanoscale particles such as carbon nanotubes (hereafter – CNTs), is one of the most rapidly developing areas of nanomaterial technology. Polypropylene (hereafter – PP), polyethene (hereafter – PE), and epoxy resins (hereafter – ER) are some of the most common environmentally friendly polymers and form a significant class of universal thermoplastics[10]. Recently, there has been increased interest in the potential of regulating the structure and properties of ER, PP, and PE with nanofillers of various natures and organizations, which determine the interaction between them and the polymer. This has resulted in the ability of composites to acquire high operational characteristics. Multi-walled carbon nanotubes (hereafter – MWCNTs) have become increasingly popular as fillers for a wide range of polymers, including ER, PP, and PE, due to their unique mechanical, electrical, and thermal properties at a low cost[19]. CNTs tend to aggregate into bundles and clumps, making uniform distribution in polymer matrices challenging. The uneven distribution of CNTs and their limited interaction with the matrix, the mechanical and kinetic properties of polymer-CNT composites are lower than expected[20].

A melt of isotactic PP from CNTs (21060 TU 05-1756-78 grade), the weight percent of which varied from 0.05 to 5.0 wt%, was stirred using the LGP-25 extruder at a speed of 50 rpm. Primary specimens were in the form of granules, which were then crushed, pressed at a temperature of 180 °C and under a pressure of 5 MPa, and extracted into fibers. The viscosity (η) of the melts of the original PP and the PP-CNT system was determined by MV-2 micro viscometer in the range of shear stresses $\tau = (0.1\text{-}5.7)\times 104$ Pa at temperatures of 190, 210, and 220 °C. Elastic properties were assessed by the extrudates' swell value (B). The assigned experimental error in determining η and B constituted ±(2÷5)%. The flow mode "n" was equal to the slope of the flow curve touching the abscissa at a given point.

The longitudinal deformation of the melt was assessed by the value of the maximum jet drawing (Fmax), where the assigned error was ±7%. The differential thermal and gravimetric analyses helped to study the crystallization behavior of PP in CNT composites (derivatograph Q 1500, heating rate 10 degrees per minute). The dependence of the specific thermal conductivity of the specimens on temperature was measured by the dynamic heating method using an IT-400 industrial device equipped with an analog-digital device for recording data on a personal computer. The specimens were coated with a thin layer of graphite lubricant to improve thermal contact with the measuring plates. During measurements, the temperature varied from 40 to 170 °C, and the heating rate was 5 °C/min. The relative error of the method was ±5%. The specimens had a cylindrical shape with a diameter of 15 mm and a height of 1.3-1.7 mm.

E7-14 LCR meter was used to examine electrical conductivity at low frequencies at room temperature by the two-contact method. Compression or rupture of fibers was tested using a 2167-P50 tensile testing machine in the repeated-static compression mode; a strain diagram was recorded until the final destruction of the specimen. The fibers were fixed by winding on cylindrical clamps, where the loading speed was 10 mm/min.

CNTs were produced by the catalytic chemical vapour deposition (CCVD) through ethylene, propylene or propane butane pyrolysis on complex metal oxide catalysts. These catalysts were obtained by precipitation or aerosol evaporation of water-soluble salts of iron or nickel, aluminium, and molybdenum. The CNT synthesis was carried out using the equipment with a reactor of 30 dm3 and an output of about 1.5kg of product per day. According to the standard of Ukraine, the average diameter of CNTs was 10-20nm, while the specific surface defined by the argon desorption was 200-400m2/g, and the bulk density was within 20-40 g/dm3. According to the data of the transmission electron microscopy (TEM), X-ray diffraction, combined scattering spectroscopy, and differential thermal and gravimetric analyses, no amorphous carbon was found.

CNTs were introduced into the epoxy resin by mixing in a three-roll viscous liquid mixer. Three types of influence of curing conditions were established, including curing without external influence, curing under pressure, and curing with vacuum pumping.

3. Results

The structural properties and crystallization reactions of composites, as well as their dependence on carbon nanotube concentration, were studied using differential thermal analysis (hereafter – DTA), differential thermogravimetric analysis, and X-ray diffraction methods. The DTA analysis results of samples that differed only in filler concentration are presented in Table 1, which includes the temperatures at the beginning and end of the melting and crystallization processes, the temperature range of these processes, and the temperature of the DTA peak extremum.

Table 1. Characteristic temperatures of melting, crystallization processes, and degree of crystallinity determined for the PP-CNT system with varying filler concentrations.

No.	PP-CNT System	Melting Process				Crystallization Process				Degree of Crystallinity (%)
		T_{start} °C	T_{peak} °C	T_{end} °C	ΔT, °C	T_{start} °C	T_{peak} °C	T_{end} °C	ΔT, °C	
1	PP	143	170	190	47	126	116	106	20	71.0
2	PP + 0.05%	143	171	192	49	128	122	107	21	71.8
3	PP +0.1%	142	171	189	47	130	122	110	20	61.0
4	PP +0.5%	140	172	190	50	130	120	112	18	63.6
5	PP +1%	145	170	190	45	134	126	116	18	63.9
6	PP +3%	144	170	192	48	137	128	116	21	64.6
7	PP +5%	147	172	188	41	138	131	117	21	68.2

Table 1 shows that the melting process's characteristic temperatures depend on the presence of CNTs and change non-monotonically as their concentration in the composite increases. For example, the lowest temperature at the start and the highest temperature range of the melting process are observed in the PP-CNT system with a CNT content of 0.5% (by weight). The limited mobility of the polymer chains, possibly due to interactions between the polymer and the filler's surface, is the cause of the increase in melting and crystallization temperatures with increasing CNT content in the polymer.

Within the investigated concentration range, there is a monotonic but nonlinear increase in characteristic temperatures as CNT concentration increases. It is important to note that the minimum crystallization temperature at a concentration of 0.5% (by weight) CNTs is 120 °C.

The obtained data for the PP-1.0 wt% composite with CNTs is in good agreement with the results for the PP composite containing 0.8 wt% single-walled CNTs (hereafter – SWCNTs): the crystallization temperature in the PP-SWCNT system increases, and the temperature interval (ΔT) for melting and crystallization is smaller compared to pure PP. This suggests that single-walled and multi-walled CNTs have a similar influence on the structural formation processes of composites.

The X-ray diffraction patterns of samples from the core and edge of PP-CNT composites with CNT concentrations of 0.5, 1.0, 3.0, and 5.0 wt% are shown in Figure 1. It should be noted that the X-ray diffraction pattern is devoid of prominent reflections corresponding to CNTs' graphite-like structure. The overall appearance of the X-ray diffraction indicates that the polymer in the composite, like the pristine PP, has a typical -form of crystals, which is supported by DTA melting temperature data.

Figure 2 depicts the decomposition of the X-ray diffraction spectrum into components. It is attributed to both crystalline and amorphous phases, indicating non-monotonic changes in the concentration of the topologically ordered phase with increasing CNT content. At the lowest CNT concentration (0.05% by weight), there is a slight increase in crystallinity (71.8%) compared to the original PP, which has a crystallinity of 71%. However, at a CNT content of 0.1% by weight, the crystallinity drops to 61%.

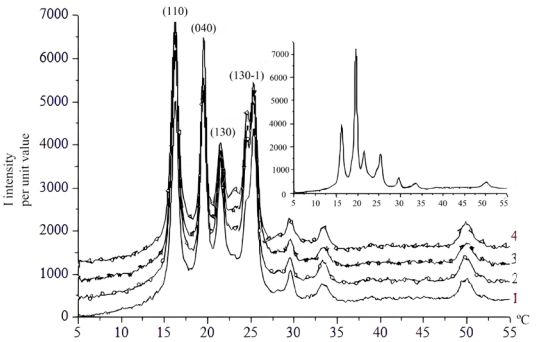

Figure 1. X-ray diffraction of PP-CNT samples with different CNT concentrations.

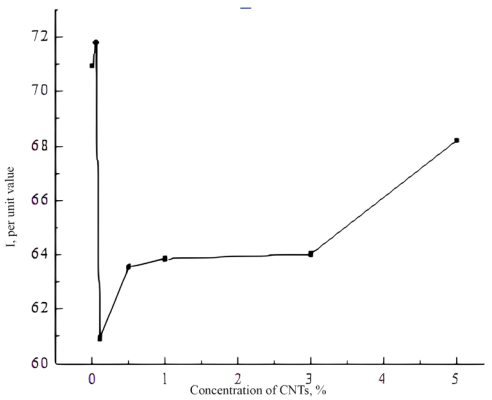

Figure 2. Dependence of the degree of crystallinity determined from X-ray structural data on the CNT concentration in the PP-CNT system.

Furthermore, as CNT concentration increases to 3%, the degree of crystallinity increases to 64.4%, and at 5% concentration, it reaches 68.2% (Figure 2). This qualitatively correlates with changes in the onset of crystallization temperature (Table 1) and the dependence of the half-width of the X-ray reflexes on CNT concentration in the PP-CNT system (Figure 3), where they decrease or remain unchanged at a concentration of 0.05% by weight, then increase in the concentration range of 0.1% to 0.5% by weight of CNTs.

The specified concentration range, as demonstrated by DTA and electron X-ray diffraction methods, is characterized by a reduced degree of crystallinity compared to the original polymer, resulting in a significant amount of unordered phase and the presence of nanopores, which contribute to a decrease in the composite's thermal conductivity by reducing the polymer's thermal conductivity and additional energy scattering. The additive contribution of a more thermally conductive component of the composite compensates for the increase in thermal conductivity with an increase in filler content. The presence of the polymer-CNT interphase boundary impedes the achievement of thermal conductivity values comparable to CNT with the energy loss of phonons due to the low conductivity of the contacts being the determining factor[13,19-22].

An inverse relation between the amount of nanomodifier absorbed and cone slump is observed when introducing CNTs into a concrete mixture. Increasing the amount of CNTs absorbed decreases this relation but increases the loss of mobility. When polyelectrolyte molecules are rapidly absorbed by positively charged minerals of Portland cement clinker and hydration products, an amount of nanomodifier in the liquid phase of the concrete mixture remains insufficient to maintain mobility at a given level. The amount of the nanomodifier absorbed by various monominerals of Portland cement clinker and mineral additives was determined to examine the mobility properties of cement pastes after the introduction of CNTs. The following materials were used: monominerals of Portland cement clinker, Portland cement (activity 525 kgf/cm^2), and CNT nanomodifier.

The authors studied how the type of dispersion medium affects the efficiency of uniform CNT distribution in a laboratory disperser (dispersion duration was 60 minutes). The medium dispersity was assessed on the kinetics of CNT sedimentation prepared in a disperser. The highest sedimentation rate was observed when tap water was used as a liquid medium. The sedimentation rate decreased in a superplasticizer solution, indicating a more homogeneous dispersion composition. The lowest sedimentation rate was observed in the polymer solution with highly concentrated alkaline agents; thus, this medium provided for the most uniform nanomodifier distribution and the formation of stable colloidal particles. When the amount of alkali is minimal, CNTs can polymerize, and a suspension should be used as a precursor. The degree of CNT distribution is exclusively influenced by suspension self-heating temperature during dispersion, which is achieved mainly through friction work. An increase in temperature intensifies the distribution process, primarily due to a decrease in the suspension's viscosity.

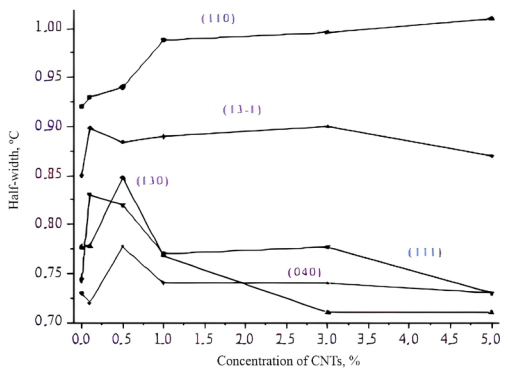

Figure 3. Dependence of the half-width of X-ray reflections of PP on the CNT concentration in the PP-CNT system.

4. Discussion

After examining the chemical changes in composites, the mechanical properties of the PP-CNT system were investigated. The presence of CNTs in the composite has no effect on the stress-strain curve, as shown in Figures 4a and 4b, which show compression curves for PP and the PP-5% CNT composite; it only changes the quantitative values of the characteristics. The curves display typical rigid polymer behaviour. However, adding 5% CNTs to PP significantly increases tensile strength (by 55%) while decreasing fracture

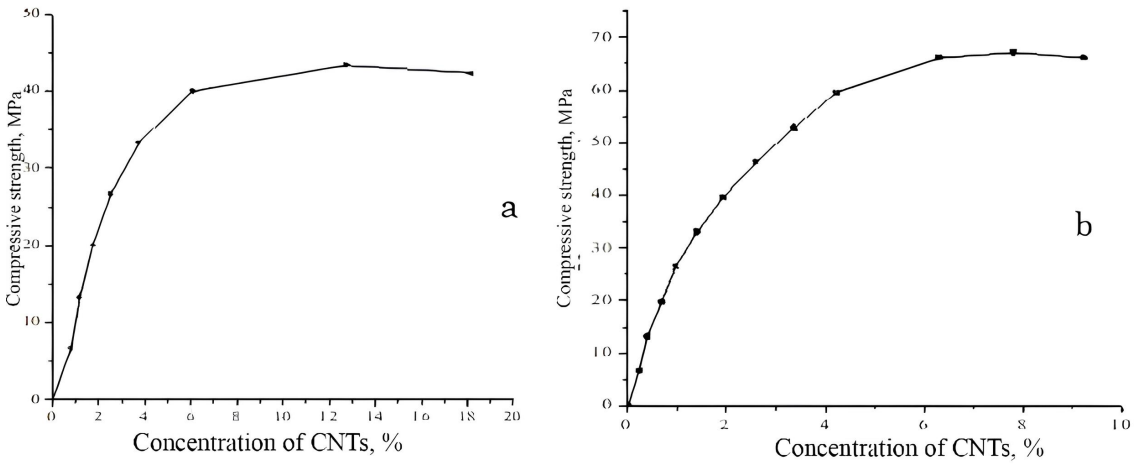

Figure 4. Compression diagrams for pure PP (a) and PP+5% CNT composite (b).

strain by about 40%. When CNTs are added, the fracture strain decreases during compression, indicating that the polymer's brittleness increases.

Figures 5 and 6 show how deformation and compressive stress are affected by the concentration of CNTs in the composite.

The compressive strain appears to decrease sharply at a concentration of 0.5% mass (material becomes more brittle) and then gradually increases with increasing CNT concentration but remains lower than that of pure PP. As a result, in terms of character, the dependence of compressive strain on CNT concentration is similar to the dependence of kinetic characteristics on CNT concentration and correlates with the dependency of the degree of crystallinity in the PP-CNT system on CNT concentration. The compressive strain is reduced by amorphization of the polymer structure, and its value gradually increases after the emergence of a continuous CNT network.

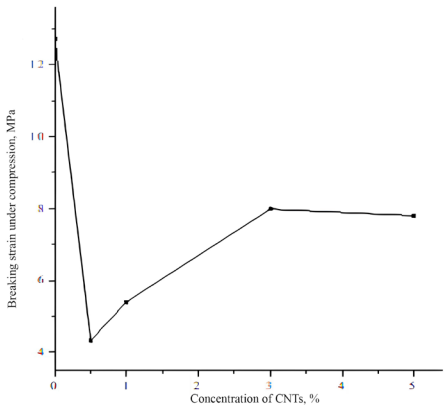

Figure 5. Dependence of compressive deformation on the concentration of CNTs in PP-CNT composites.

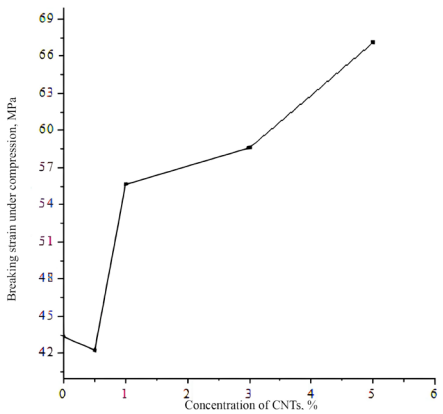

Figure 6. Dependence of compressive strength on the concentration of CNTs in PP-CNT composites.

The compressive strength decreases slightly at 0.5% mass CNT concentration and then increases significantly after passing a certain threshold, surpassing the value for pure PP.

The increase in deformation is associated with a decrease in the frequency of chemical cross-linking within the network. However, the decrease in modulus is compensated for by an increase in modulus due to improved bonding between the surface of functionalized CNTs and the polymer matrix, which involves the formation of covalent bonds between functional groups and epoxy cycles. Data from studies of various researchers[7,20-27] reveals that compared the efficiency of modification using different types of nanotubes (Table 2) provide support for this hypothesis.

The analysis of the presented findings demonstrates that modification with the original nanotubes results in an increase in modulus and a decrease in relative elongation. Non-functionalized nanotubes thus serve as a typical high-modulus filler. When epoxy systems are modified with nanotubes functionalized with amino groups, the modulus of elasticity and the elongation of the epoxy composites increase simultaneously. Based on the data presented, it is possible to conclude that carbon nanotubes, in addition to reinforcing the oligomer, can influence the change in physical and mechanical properties by participating in the curing process and forming the structure of the polymer matrix.

The development of high-temperature binders for structural polymer composite materials (hereafter – PCMs) is one of the current challenges in materials science. The traditional method of creating binders with the highest density of chemical crosslinks does not always produce the desired results. The glass transition temperature increases as the crosslink density rises, but this results in decreased tensile strain and impact resistance of the polymer matrix, which has a negative impact on the properties of PCMs[27]. The strength of the bonded polymers is determined by the balance between the frequency of crosslinks, which increases the elastic modulus and glass transition temperature, and the number of physical network nodes providing one-dimensional stress redistribution due to relaxation processes. As a result, with the same number of physical network nodes, increasing the frequency of crosslinks increases strength; however, once the frequency of crosslinks is high enough to freeze relaxation processes, the strength decreases. Several examples of developments are provided below to demonstrate a potential solution to this problem. Based on the assumptions about the carbon composites (hereafter – CNCs) modification mechanism described above, a strategy for using carbon nanotubes to modify high-temperature binders based on epoxy matrices

Table 2. Comparison of the physical and thermomechanical properties of composites.

	Temperature, °C	Elastic modulus in tension, GPa	Relative deformation, %
Initial	170.15	2.0	5.4
0.5% MWCNT	164.64	2.3	4.6
0.1% MWCNT	158.35	3.35	7.25

was developed. The binder was first synthesized as a precursor using ED-20 resin, 4,4-diaminodiphenylsulfone hardener, and multi-walled functionalized carbon nanotubes (hereafter – FWCNTs). FWCNTs were ultrasonically dispersed in acetone to prepare the precursor. The resin and hardener were then added to the dispersion in a stoichiometric ratio and stirred for 40 minutes. Vacuum was used to remove the remaining solvent. The obtained precursor was added to the standard binder at a rate of 25 parts by weight per 100 parts by weight of the binder in terms of the dry residue, stirred with a magnetic stirrer, and the viscosity of the modified system was adjusted to the required technological level[21]. The binder-modified impregnated carbon tape was dried for 5 days. The PCM was pressed in step mode (temperature 120 °C, 30 minutes soaking, temperature 180 °C, 25 atm pressure, 4 hours soaking). As can be seen from the data, as the concentration of FWCNTs increases, so do the glass transition temperature and dynamic modulus of elasticity, reaching a maximum at a concentration of CNCs ≈ 0.13 mass% and monotonically decreasing beyond this concentration.

Table 3 demonstrates the dependencies of glass transition temperatures and dynamic elastic moduli of unidirectional polymer composite materials (PCMs) based on ENFB-2M and VS-2526K binders with the addition of a modified precursor ED-20/4,4-diaminodiphenylsulfone, modified with 0.13 wt.% FMWNT (Functionalized Multi-Walled Carbon Nanotubes). PCMs based on these binders containing no carbon nanotubes (CNTs) were used as reference samples. The addition of the modified precursor FBWNT to the composite allows for an increase in the glass transition temperature of PCMs of 14 and 8 °C, respectively, as well as an increase in the elastic modulus of the ENFB-2M and VS-2526K binders of 23 and 11%. The formation of more frequent and regular cross-linking networks in the presence of CNTs is likely to be associated with improved thermomechanical properties.

Presumably, the increase in the frequency and regularity of chemical cross-linking networks explains the overall improvement in the properties of PMC (polymer matrix composites) reported by abovementioned authors[7,22-28]. The astralen modifiers were used in this study.

The corrosion resistance of CNT-modified concretes was determined on 0.04×0.04×0.16 m prism specimens. The results of these studies are presented in Table 4.

The analysis of the results of specimen frost resistance showed that nanomodified concretes have high corrosion resistance to various aggressive media, including acids. CNT-modified concrete specimens of composition No. 1 (separate preparation technology), aging for six months in

Table 3. Thermodynamic properties of PCM with different types of compounds.

No.	The composition's components	Mass concentration of CNT %	Elastic modulus MPa	Glass transition temperature °C
1.	EPHB-2M	0	57800	185
2.	EPHB-2M+25%	0	60400	177
3.	EPHB-2M+25% ED20/DAFCS+UNT	0.13	71420	199
4.	VC-2526K	0	78000	165
5.	VC-2526K+25% ED20/DAFCS	0	74000	163
6.	VC-2526K+25% ED20/DAFCS+UNT	0.13	87000	172

Table 4. Change in mass and strength of nanomodified concrete specimens under alternate freezing and thawing.

No.	Frost resistance criteria											
	Increase (+) and decrease (-) in ultimate compressive strength under alternate freezing and thawing, %						Mass loss, %					
	Number of cycles											
	100	150	200	250	300	350	100	150	200	250	300	350
Composition No. 1	+4.0	+1.2	+0.5	-1.5	-2.7	-3.2	0	0	0	0	0	0.2
Composition No. 2	+4.1	+1.2	0.4	-1.7	-4.2	-5.0	0	0	0	0	0	0.3
No.	**Frost resistance criteria**											
	Visual signs of failure (cracking, scaling, cleaving)											
	100		150	200	250		300	350				
Composition No. 1		no							Surface scaling			
Composition No. 2		no							no			

an aggressive medium (a solution of magnesium sulfate and sodium sulfate with a 5% concentration) showed a slight decrease in the corrosion resistance coefficient, respectively, to values of 0.89 and 0.90. The destruction of specimens aging in a hydrochloric acid solution was less intensive; the corrosion resistance coefficient decreased to 0.87. Traditionally prepared concretes also showed resistance to the development of type 3 corrosion. There was virtually no reduction in the tensile strength of concrete when aging concrete specimens in a hydrochloric acid solution (Figures 7 and 8).

CNT-modified concrete also showed higher indicators for electrocorrosion and thermal conductivity. Furthermore, the modulus of elasticity and shrinkage of concrete increased during curing.

5. Conclusions

It has been demonstrated that incorporating carbon nanotubes into a polymer matrix improves the physicochemical, physicomechanical, and operational properties of composite nanopolymer materials. The physicomechanical properties of polymer composites reinforced with carbon nanotubes improve by 30-40%. When creating structural polymer composite materials, functionalized carbon-containing nanoparticles can be used as modifiers to control the curing process and elasticity of epoxy materials.

The investigated possibility of using nanoparticle self-organization to impart functional properties to composite materials and to obtain 3-D reinforced hybrid nanocomposites has shown its effectiveness. The diversity of allotropic forms and unique geometric carbon nanosized objects provide for designing radio-absorbing fillers with the necessary ratio between the real and imaginary parts of the permittivity.

Based on the research and the experimental results obtained, prototypes of the elements of an unmanned aerial vehicle ("engine cowlings") were manufactured using improved technology that involved introducing CNTs in an optimal amount to the epoxy matrix. Nanotubes give the element a black color, while the black element does not allow determining the distance to it using a Laser rangefinder monocular LRM1500M at a range of over 100 m. This laser rangefinder can determine the distance to an object within 10-1500 m.

Contemporary advancements in the field of composites are devoted to the creation of materials based on both carbon fillers and carbon nanotubes. However, due to the specifics of the source materials and the properties of carbon nanotubes, as well as the need for cost-effective production, modern processes are receiving the most attention. As a result, scientists and engineers are expected to devote significant attention to the development of new binders for the production of composites. Innovative construction materials open up new prospects for sustainable development of the industry. The use of CNT nanomaterials helps to create durable, energy-efficient, and environmentally friendly structures. The development and implementation of these innovations is an important step towards sustainable development of economic activity, which will help ensure a comfortable life for future generations.

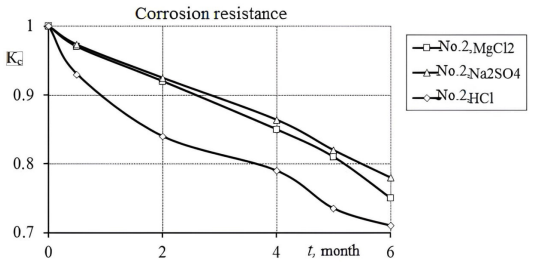

Figure 7. Dependence of the corrosion resistance coefficient of concrete (composition No. 1) on aging in an aggressive medium.

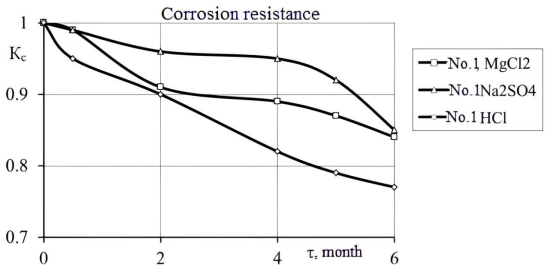

Figure 8. Dependence of the corrosion resistance coefficient of concrete (composition No. 2) on aging in an aggressive medium.

6. Author's Contribution

- **Conceptualization** – Olena Bakulich.
- **Data curation** – Andrii Bieliatynskyi.
- **Formal analysis** – Mingyang Ta.
- **Funding acquisition -** Andrii Bieliatynskyi.
- **Investigation** – Mingyang Ta.
- **Methodology** – Viacheslav Trachevskyi.
- **Project administration** – Andrii Bieliatynskyi.
- **Resources** – Olena Bakulich.
- **Software** – Mingyang Ta.
- **Supervision** – Viacheslav Trachevskyi.
- **Validation** – Andrii Bieliatynskyi.
- **Visualization** – Mingyang Ta.
- **Writing – original draft** – Olena Bakulich.
- **Writing – review & editing** – Viacheslav Trachevskyi.

7. Acknowledgements

The authors gratefully acknowledge the financial support from the Science and Technology Department of Ningxia, the Scientific Research Fund of North Minzu University (No. 2020KYQD40).

8. References

1. Restuccia, K. L., Hobisch, G., Jacobs, V., & Ponsolle, D. (2020). *US Patent No 10,655,006.* Washington: U.S. Patent

and Trademark Office. Retrieved in 2024, October 28, from https://patentimages.storage.googleapis.com/de/1a/82/cf74605bde8653/US10655006.pdf

2. Bieliatynskyi, A., Yang, S., Pershakov, V., Shao, M., & Ta, M. (2023). Study of concrete properties based on crushed stone sand mixture and fibre of fly ash of thermal power plants. *Science and Engineering of Composite Materials*, *29*(1), 412-426. http://doi.org/10.1515/secm-2022-0167.
3. Grand View Research. (2023). *Composites market size, share & trends analysis report by product type (carbon fiber, glass fiber), by manufacturing process (layup, filament, injection molding, pultrusion), by end-use, by region and segment forecasts, 2023-2030.* San Francisco, CA: Grand View Research. Retrieved in 2024, October 28, from https://www.grandviewresearch.com/industry-analysis/composites-market
4. Yang, S., Bieliatynskyi, A., Trachevskyi, V., Shao, M., & Ta, M. (2022). Technological aspects of the preparation of polymer composites of building materials and coatings. *Polymers & Polymer Composites*, *30*. http://doi.org/10.1177/09673911221135690.
5. Murray, R. E., Beach, R., Barnes, D., Snowberg, D., Berry, D., Rooney, S., Jenks, M., Gage, B., Boro, T., Wallen, S., & Hughes, S. (2021). Structural validation of a thermoplastic composite wind turbine blade with comparison to a thermoset composite blade. *Renewable Energy*, *164*, 1100-1107. http://doi.org/10.1016/j.renene.2020.10.040.
6. Wu, W., Jiang, B., Xie, L., Klunker, F., Aranda, S., & Ziegmann, G. (2013). Effect of compaction and preforming parameters on the compaction behavior of bindered textile preforms for automated composite manufacturing. *Applied Composite Materials*, *20*(5), 907-926. http://doi.org/10.1007/s10443-012-9308-1.
7. Fan, Z., Tang, W., Hsiao, K.-T., & Advani, S. G. (2004). *Flow and dispersion of multi-walled carbon nanotubes in polymer and fiberglass reinforced polymer composites.* In *Proceedings of the NSF Design, Service and Manufacturing Grantees and Research Conference.* Dallas, TX: National Science Foundation.
8. Ponsolle, D., Restuccia, K. L., Jacobs, W., Blackburn, R., LoFaro, C., Price, R., Doyle, M., Smith, M., & Roman, M. (2013). *WO 2013/096377 A2.* Geneva: World Intellectual Property Organization. Retrieved in 2024, October 28, from https://patentimages.storage.googleapis.com/c8/50/0a/0cb4772a1fb96c/WO2013096377A2.pdf
9. Kim, C., Yun, M.-G., Kim, S., & Jeon, G.-W. (2022). Mathematical model to predict the moduli of wet-laid pulp/fibre/resin composite materials. *International Journal of Precision Engineering and Manufacturing*, *23*(11), 1315-1324. http://doi.org/10.1007/s12541-022-00700-8.
10. Biron, M. (2018). *Thermoplastics and thermoplastic composites*. Norwich, UK: William Andrew. http://doi.org/10.1016/C2017-0-01099-6.
11. Bongiorno, F., Militello, C., & Zuccarello, B. (2022). Mode I translaminar fracture toughness of high-performance laminated biocomposites reinforced by sisal fibres: accurate measurement approach and lay-up effects. *Composites Science and Technology*, *217*, 109089. http://doi.org/10.1016/j.compscitech.2021.109089.
12. Giuliani, P. M., Giannini, O., & Panciroli, R. (2022). Characterizing flax fibre-reinforced bio-composites under monotonic and cyclic tensile loading. *Composite Structures*, *280*, 114803. http://doi.org/10.1016/j.compstruct.2021.114803.
13. Inam, F., Wong, D. W. Y., Kuwata, M., & Peijs, T. (2010). Multiscale hybrid micronanocomposites based on carbon nanotubes and carbon fibres. *Journal of Nanomaterials*, *2010*(1), 453420. http://doi.org/10.1155/2010/453420.
14. Kochi, S., Yoshio, K., & Miyoshi, M. (2015). *US Patent No 9,062,203.* Washington: U.S. Patent and Trademark Office. Retrieved in 2024, October 28, from https://pubchem.ncbi.nlm.nih.gov/patent/US-9062203-B2
15. Liu, Y.-N., Yuan, C., Liu, C., Pan, J., & Dong, Q. (2019). Investigation of the resin infusion process based on automated fiber placement preform. *Scientific Reports*, *9*(1), 7440. http://doi.org/10.1038/s41598-019-43982-1. PMid:31092893.
16. Loeliger, A., Yang, E., & Bomphray, I. (2021). *An overview of automated manufacturing for composite materials.* In *Proceedings of the 26th International Conference on Automation and Computing (ICAC)* (pp. 1-6), Portsmouth, UK. New York: IEEE. http://doi.org/10.23919/ICAC50006.2021.9594159.
17. Mei, M., Sun, L., He, Y., Li, M., Duan, S., Wei, K., & Yang, X. (2021). Preforming characteristics in the compaction process for fabric with binder under elevated temperature. *Composites Communications*, *23*, 100545. http://doi.org/10.1016/j.coco.2020.100545.
18. Zhao, X., Copenhaver, K., Wang, L., Korey, M., Gardner, D. J., Li, K., Lamm, M. E., Kishore, V., Bhagia, S., Tajvidi, M., Tekinalp, H., Oyedeji, O., Wasti, S., Webb, E., Ragauskas, A. J., Zhu, H., Peter, W. H., & Ozcan, S. (2022). Recycling of natural fiber composites: challenges and opportunities. *Resources, Conservation and Recycling*, *177*, 105962. http://doi.org/10.1016/j.resconrec.2021.105962.
19. Huang, Y., Li, N., Ma, Y., Du, F., Li, F., He, X., Lin, X., Gao, H., & Chen, Y. (2007). The influence of single-walled carbon nanotube structure on the electromagnetic interference shielding efficiency of its epoxy composites. *Carbon*, *45*(8), 1614-1621. http://doi.org/10.1016/j.carbon.2007.04.016.
20. Bieliatynskyi, A., Yang, S., Pershakov, V., Shao, M., & Ta, M. (2023). Exploring the use of modern fly ash materials from Chinese power plants in road and airfield infrastructure. *Environmental Engineering and Management Journal*, *22*(3), 527-537. http://doi.org/10.30638/eemj.2023.041.
21. Chandrasekaran, V. C. S., Advani, S. G., & Santare, M. H. (2010). Role of processing on interlaminar shear strength enhancement of epoxy/glass fibre/multi-walled carbon nanotube hybrid composites. *Carbon*, *48*(13), 3692-3699. http://doi.org/10.1016/j.carbon.2010.06.010.
22. Fan, Z., Hsiao, K.-T., & Advani, S. G. (2004a). Experimental investigation of dispersion during the flow of multi-walled carbon nanotube/polymer suspension in fibrous porous media. *Carbon*, *42*(4), 871-876. http://doi.org/10.1016/j.carbon.2004.01.067.
23. Qiu, J., Zhang, C., Wang, B., & Liang, R. (2007). Carbon nanotube integrated multifunctional multiscale composites. *Nanotechnology*, *18*(27), 275708. http://doi.org/10.1088/0957-4484/18/27/275708.
24. Challa, R. K., Kajfez, D., Demir, V., Gladden, J. R., & Elsherbeni, A. Z. (2008). Characterization of multi-walled carbon nanotube (MWCNT) composites in a waveguide of square cross-section. *IEEE Microwave and Wireless Components Letters*, *18*(3), 161-163. http://doi.org/10.1109/LMWC.2008.916776.
25. Huang, Q., Holland, T. B., Mukherjee, A. K., Chojnacki, E., Liepe, M., Mallory, M., & Tigner, M. (2009). *Carbon nanotube RF absorbing materials.* In *Proceedings of the 14th International Conference on RF Superconductivity (SRF2009)* (pp. 648-651). Berlin: Helmholtz-Zentrum Berlin für Materialien und Energie.
26. Lubineau, G., & Rahaman, A. (2012). A review of strategies for improving the degradation properties of laminated continuous-fibre/epoxy composites with carbon-based nanoreinforcements. *Carbon*, *50*(7), 2377-2395. http://doi.org/10.1016/j.carbon.2012.01.059.

27. Li, N., Huang, Y., Du, F., He, X., Lin, X., Gao, H., Ma, Y., Li, F., Chen, Y., & Eklund, P. C. (2006). Electromagnetic interference (EMI) shielding of single-walled carbon nanotube epoxy composites. *Nano Letters*, *6*(6), 1141-1145. http://doi.org/10.1021/nl0602589. PMid:16771569.

28. De Vivo, B., Guadagno, L., Lamberti, P. R. R., Sarto, M. S., Tamburrano, A., Tucci, V., & Vertuccio, L. (2009, June 11-12). *Electromagnetic properties of carbon nanotube/epoxy nanocomposites.* In *Proceedings of the EMC Europe 2009 Workshop: Materials in EMC Applications* (pp. 9-12), Athens, Greece. New York: IEEE. http://doi.org/10.23919/EMC.2009.10814044.

Received: Oct. 28, 2024
Revised: Jan. 31, 2025
Accepted: Apr. 17, 2025